1

Introduction

Understanding and describing particulate processes requires knowledge about the micro-mechanical behavior of the granular materials. In many industries, such as chemical, pharmaceutical and food technology, particles are processed or produced for example in mixers, fluidized beds and spray dryers. These processes are characterized by intense multiple contacts between particles and between particles and the apparatus walls. Hereby, a change in micro-mechanical collision dynamics strongly influences the macroscopic behavior of a fluidized bed, as for example van Buijtenen et al. (2009) showed. Therefore, knowing the collision dynamics is important, when designing particulate processes.

During a collision of particles different adhesive effects can lead to a change of collision behavior by reducing the kinetic energy of the particles. Rumpf (1958) and Schubert (1979) divide adhesive effects into two different categories: Adhesive mechanisms with and without material bridges are distinguished. Surface and field forces between close or contacting particles, such as van der Waals, electrostatic and magnetic forces, as well as interlocking mechanisms are associated to adhesion without material bonds. Van der Waals forces result from dipole moments of the molecules a particle consists of. They are always active but depend strongly on the type of material and only have a small spatial range, where they can lead to adhesion. Electrostatic forces only act, if the particles are electrically charged for example due to static friction (Rumpf, 1958), while magnetic forces require magnetic materials and fields. Interlocking of materials occurs for example if fibres or surface roughness peaks overlap and interlock (Tomas, 2007). These interlockings have to be broken before the particles can rebound leading to higher energy dissipation and smaller rebound velocities. Adhesion with material bridges represent for example forces due to adsorption layers, liquid bridges between surface wet particles or solid bonds formed via sintering or crystallization of solvents from liquid bridges.

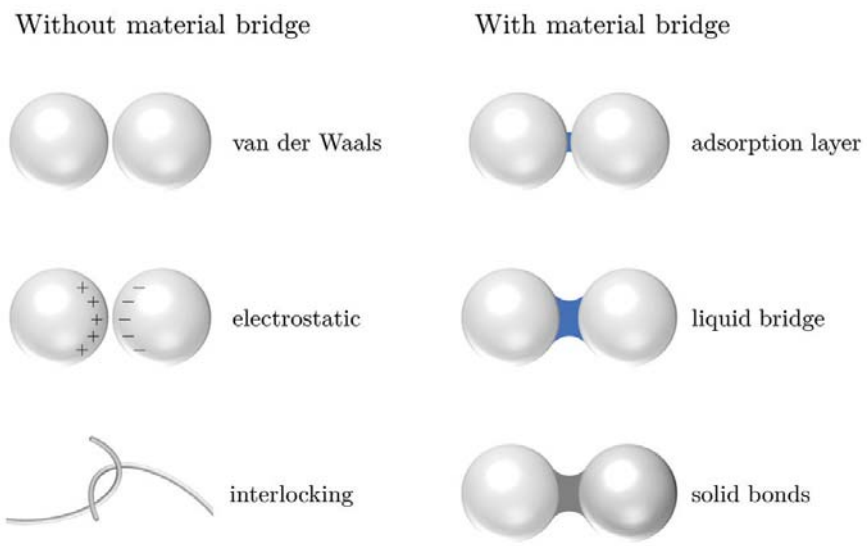

FIGURE 1.1: Mechanisms of adhesion after Rumpf (1958) and Schubert (1979).

Adhesion due to liquid bridges and layers between particles are of special interest, because in many industrial processes particles are wet before or wetted while being processed. For instance during granulation or agglomeration of particles, liquids are injected into the apparatus. The liquids deposit on the particle surfaces and lead to a growth in particle size. This particle size enlargement strongly depends on the collision dynamics and in particular on the influence of the injected liquids on collision behavior: When wet particles collide with each other or the apparatus walls, the particles might stick together due to adhesive forces of the liquid bridge forming between the surfaces. This would lead to formation of agglomerates. If the particles do not stick, but instead rebound from each other, the liquid droplets or layers on the particles can dry off. When the liquid consist of a melt or suspension, the dryed solid results in a slow layer by layer growth of the particles.

For the design of industrial processes it is important to know a priory, if particles stick and form agglomerates or if they rebound. An universal correlation to predict rebound behavior of wet particles or a physical description of the impact and rebound dynamics is still missing though. The aim of this thesis is to provide a physical understanding of the influence of liquid layers on collision dynamics of wet particles, focusing on the influence of the liquid properties, the particle attributes and the collision parameters. Therefore, rebound behavior of particles impacting on walls covered by liquid layers is investigated experimentally as well as using a force balance model. After summarizing previous knowledge and research regarding collision dynamics of dry and wet particles, the experimental procedures as well as used force balance model are described in chapter 2. Both normal and oblique collisions of dry particles and a wet wall are studied experimentally in chapter 3 focusing on the influence of the liquid layers on energy dissipation. From these results an empirical equation is derived, which predicts rebound behavior

of the particles in the investigated range of parameters. Subsequently, the proposed force balance model is compared to experimental results and thus validated in chapter 4. Since this force balance is based on physical principles the experimental parameter range is extrapolated numerically to values, which are difficult to investigate experimentally or have been rarely analyzed before. Thereby, an even deeper understanding of collision dynamics is possible. The system of a dry particle colliding with a wet wall still has some simplifications compared to particle - particle collisions. Therefore, chapter 5 gives first impressions on particle - particle collisions by investigating the difference of collisions, where either the wall, the particle or both, particle and wall, are wet before the collision experimentally. Afterwards, dry and wet particle - particle collisions are investigated numerically via the force balance model. Possible differences and additional effects found numerically for particle - particle impacts compared to the previous results of particle - wall collisions will be pointed out. Finally, in chapter 6 the most important results of this thesis are summarized and topics still open for further research are indicated. In the future the models developed in this thesis may be used and integrated into Discrete Element Method (DEM) simulations to investigate the influence of liquids on the dynamic behavior of larger granular systems.

1.1 General description of dry and wet collision dynamics

In the following, basics of dry collisions and additional effects due to liquid layers and bridges are described.

1.1.1 Dry collision behavior

Generally, a collision is characterized by a short contact of two (or more) bodies during which a contact force acts. The impulse due to this contact force leads to a deformation of the contact area and a resulting change in the state of motion of the bodies. In detail, a normal collision can be divided into two phases, the compression phase and the restitution phase (Antonyuk et al., 2010, Gross et al., 2010). In the compression phase the colliding bodies are compressed in the contacting area and initial kinetic energy is stored in the deformed material as internal deformation energy. During increasing deformation the contact force increases, while the relative velocity of the bodies decreases. After reaching the maximum contact force and deformation, the stored energy is released again in the restitution phase. In this phase the contact force leads to an acceleration of the contacting bodies, while deformation is reduced. In the case of rate-independent deformation at the same time as the maximum contact force occurs the relative velocity is zero.

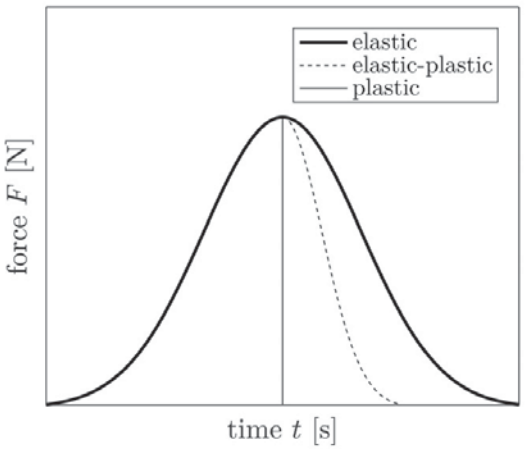

FIGURE 1.2: Schematic force-time plot for a normal collision.

During collision part of the initial deformation energy might get dissipated for example in inelastic (plastic) deformation (Kharaz and Gorham, 2000), vibration (Hunter, 1957, Weir and Tallon, 2005), friction and adhesion (Dahneke, 1975, Wall et al., 1990). Three deformation behaviors are generally distinguished: elastic, elastic-plastic and plastic behavior. In an ideal elastic collision the energy after collision is the same as before the collision, thus the relative velocity before collision equals that after the collision ($v_0 = v_\mathrm{R}$). An ideally plastic deformation behavior is characterized by dissipation of all initial energy, resulting in a rebound velocity of zero ($v_\mathrm{R} = 0$). Most real materials behave elastic-plastic, where a specific part of the initial energy gets dissipated. Therefore, the rebound velocity is smaller than the impact velocity ($v_\mathrm{R} < v_0$). The amount of energy dissipated depends among others on the material of the colliding bodies, the mechanical history of the materials and in some cases also on the collision velocity. Figure 1.2 schematically shows the force-time diagram for an elastic, plastic and elastic-plastic collision.

In addition to the deformation behavior, collisions can be differentiated by collision scenarios: A collision can happen normal or obliquely and centric or eccentric (Gross et al., 2010). A centric collision is present if the center of mass of both collision partners lies on the normal of the point of contact (see figure 1.3). In an eccentric collision this is not the case for at least one center of mass. Accordingly, a normal collision is defined as collision where all impact velocities are in the same direction as the normal of the contact area. If the velocities in the contact feature a tangential part the collision is oblique. The collision angle α of such oblique collisions is defined as angle between the collision velocity vector and the normal vector to the contact area, being zero for a normal collision.

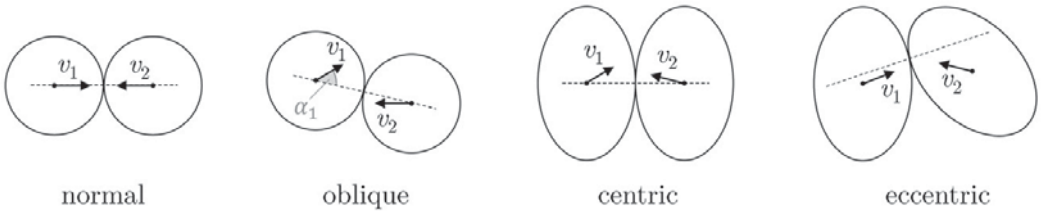

FIGURE 1.3: Different collision scenarios for a particle - particle collision.

During oblique collisions the properties of the surfaces have to be taken into account. If the surfaces can be assumed as smooth, the tangential velocity before collision is equal to that after collision ($v_{\mathrm{t,R}} = v_{\mathrm{t},0}$). However, if the surfaces are not ideally smooth, but (slightly) rough, friction takes place between the colliding surfaces. This friction leads to a change of motion in tangential direction including conversion of energy between rotational and translational movement (Luding, 1995). Depending on the ratio of normal and tangential contact forces, rough surfaces might either stick together or slide on each other. Increasing the tangential impact velocity in the contact (sum of tangential translational velocity v_{t} and rotation ω) leads to an increasing tangential contact force $F_{\mathrm{c,t}}$, which, however, is limited by Coulomb's law of friction: As long as the tangential contact force remains smaller than the product of friction coefficient μ_{fr}, which is a constant coefficient characteristic for each combination of surfaces, and the normal contact force $F_{\mathrm{c,n}}$ ($F_{\mathrm{c,t}} < \mu_{\mathrm{fr}} F_{\mathrm{c,n}}$), the surfaces stick. If the tangential impact velocity is increased above this value, the surfaces start to slide and the tangential contact force equals $\mu_{\mathrm{fr}} F_{\mathrm{c,n}}$. During sticking contact, sometimes also rolling friction has to be considered. However, in this work rolling friction is not taken into account since the investigated contacts are short and deformation small enough, that rolling can be assumed negligible.

By considering impulse and momentum balances of the collision system rebound dynamics can be calculated from the initial impact conditions:
Figure 1.4 shows the impulses $\hat{F}_{\mathrm{n}}$ and $\hat{F}_{\mathrm{t}}$ acting in normal and tangential direction on a particle colliding obliquely with a wall or another particle. For a spherical particle colliding obliquely with a wall, the wall is generally assumed immovable. Thus, only the movement of the particle is considered. The impulse in normal (n) and tangential (t) direction of the collision and the momentum can be expressed as:

$$m_{\mathrm{P}} \left(v_{\mathrm{n,R}} - v_{\mathrm{n},0} \right) = -\hat{F}_{\mathrm{n}} \tag{1.1}$$

$$m_{\mathrm{P}} \left(v_{\mathrm{t,R}} - v_{\mathrm{t},0} \right) = -\hat{F}_{\mathrm{t}} \tag{1.2}$$

$$I_{\mathrm{P}} \left(\omega_{\mathrm{R}} - \omega_0 \right) = -R_{\mathrm{P}} \hat{F}_{\mathrm{t}} \tag{1.3}$$

with I_{P} as moment of mass inertia of the particle, which is equal to $\frac{2}{5} m_{\mathrm{P}} R_{\mathrm{P}}^2$ for a sphere, as well as particle radius R_{P} and mass m_{P}. If part of the initial kinetic energy

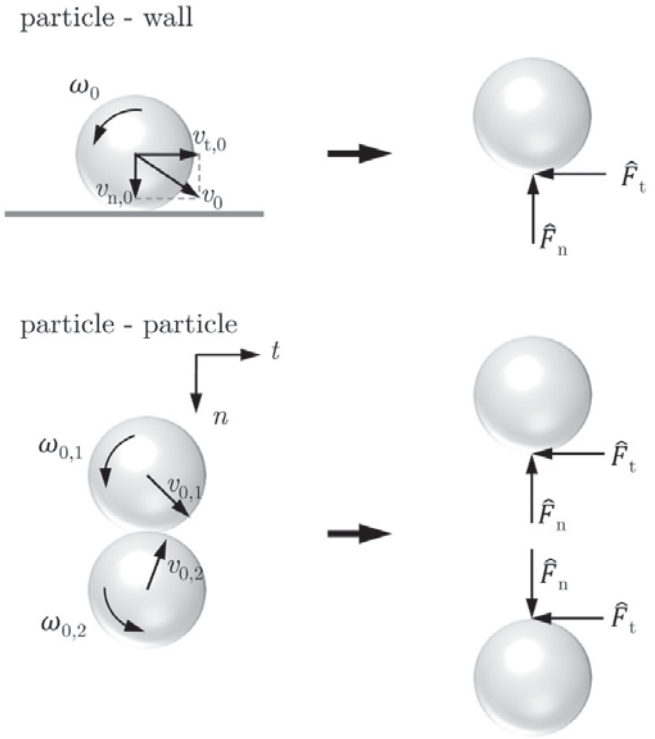

FIGURE 1.4: Impact scenarios with impulse and moments acting on colliding bodies.

of the particle is dissipated during the collision due to inelastic deformation, the normal velocities of the particle can be related to each other by

$$\frac{v_{n,R}}{v_{n,0}} = -e \tag{1.4}$$

with the so called coefficient of restitution e, which is discussed in more detail in chapter 1.2. In tangential direction the velocity in the contact point is crucial. For a collision of particles, which are not ideally smooth, often sticking of the surfaces is assumed. In this case the tangential rebound velocity in the contact $v_{R,CP}$ is zero:

$$v_{R,CP} = v_{t,R} + \omega_R = 0 \tag{1.5}$$

Using equation 1.1 to 1.5 the rebound characteristics can be solved analytically. If $|\hat{F}_t| > \mu_{fr}|\hat{F}_n|$ the particle slides on the surface and equation 1.5 is not valid. Instead, the tangential impulse can be derived from the normal impulse directly by applying equation 1.6:

$$|\hat{F}_t| = \mu_{fr}|\hat{F}_n| \tag{1.6}$$

The tangential impulse always acts in the direction opposite to the tangential movement in the contact.

For a particle - particle collision the balance of impulse and momentum can be derived according to the case of a particle - wall collision, but considering the velocities of both particles (index 1 or 2):

$$m_{\mathrm{P1}} \left(v_{\mathrm{n,R,1}} - v_{\mathrm{n,0,1}} \right) = -\hat{F}_{\mathrm{n}} \tag{1.7}$$

$$m_{\mathrm{P1}} \left(v_{\mathrm{t,R,1}} - v_{\mathrm{t,0,1}} \right) = -\hat{F}_{\mathrm{t}} \tag{1.8}$$

$$I_{\mathrm{P1}} \left(\omega_{\mathrm{R,1}} - \omega_{\mathrm{0,1}} \right) = -R_{\mathrm{P1}} \hat{F}_{\mathrm{t}} \tag{1.9}$$

$$m_{\mathrm{P2}} \left(v_{\mathrm{n,R,2}} - v_{\mathrm{n,0,2}} \right) = \hat{F}_{\mathrm{n}} \tag{1.10}$$

$$m_{\mathrm{P2}} \left(v_{\mathrm{t,R,2}} - v_{\mathrm{t,0,2}} \right) = \hat{F}_{\mathrm{t}} \tag{1.11}$$

$$I_{\mathrm{P2}} \left(\omega_{\mathrm{R,2}} - \omega_{\mathrm{0,2}} \right) = -R_{\mathrm{P2}} \hat{F}_{\mathrm{t}} \tag{1.12}$$

Equations 1.4 and 1.5 have to be modified according to:

$$\frac{v_{\mathrm{n,R,1}} - v_{\mathrm{n,R,2}}}{v_{\mathrm{n,0,1}} - v_{\mathrm{n,0,2}}} = -e \tag{1.13}$$

$$v_{\mathrm{R,CP}} = v_{\mathrm{t,R,1}} + R_{\mathrm{P1}} \omega_{\mathrm{R,1}} - v_{\mathrm{t,R,2}} + R_{\mathrm{P2}} \omega_{\mathrm{R,2}} = 0 \tag{1.14}$$

1.1.2 Additional effects during wet collisions

If liquid layers are involved in a collision additional effects due to the liquid have to be taken into account. For one the liquid adds a resistance against movement due to viscous effects. In tangential direction it furthermore acts as lubricant, reducing friction between the surfaces (Joseph and Hunt, 2004, McFarlane and Tabor, 1950a). The surface tension of the liquid also introduces adhesive or repulsive forces depending on the geometry of the liquid. Overall, according to Antonyuk et al. (2009) and Sutkar et al. (2015) a wet collision can be divided into four phases: First, penetration of the liquid layer; second, the solid-solid contact as described before; third, emergence of the colliding bodies from the liquid and fourth, the liquid bridge phase, where a liquid bridge forms between the two collision partners. The collision is assumed to be finished, when the liquid bridge ruptures and both bodies are separate again. These four phases are displayed exemplary for a normal particle - wall collision in figure 1.5. During phase one, three and four, the aforementioned viscous and capillary effects show a major influence, which will be discussed in the following.

Viscous effects result from the (viscous) damping resistance of the liquid being pushed aside by the impacting particle. The viscous resistance force due to the liquid depends mainly on the size and geometry of the liquid volume, which has to be moved aside, the velocity v of the impact as well as the viscosity η of the liquid. In literature various models were developed for different geometric and material systems. Lian et al. (1996)

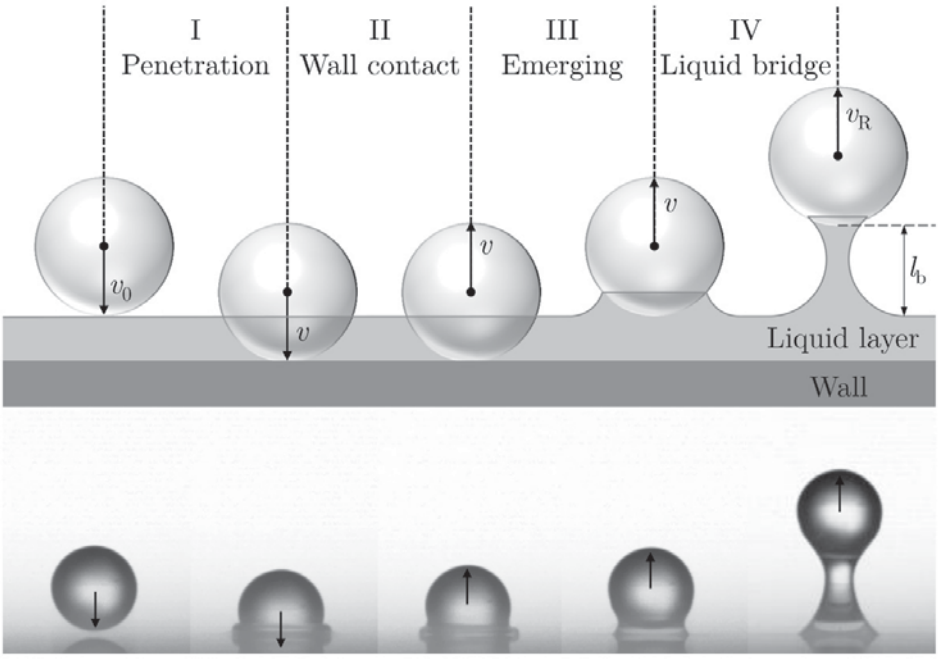

FIGURE 1.5: Phases during wet particle - wall collisions based on Antonyuk et al. (2009): Schematic (top) and experimental images (bottom).

beside others (Chan and Horn, 1985, Matthewson, 1988, Mazzone et al., 1987) use an equation for the viscous force on a spherical particle approaching another spherical particle or wall inside an infinite liquid, depending on the mean radius of the contacting bodies R and the distance of the bodies S:

$$F_{\text{vis}} = 6\pi\eta R v \frac{R}{S} \tag{1.15}$$

Besides this often cited equation, Matthewson (1988) developed a solution of the viscous force for a small liquid amount between a particle and a wall, comparable to a droplet between them. Goldman et al. (1967) investigated viscous effects of a particle moving translationally or rotationally parallel to a wall. Viscous forces for particle - particle collisions are given e.g. by Mazzone et al. (1987) and Marshall (2011). Some research is still conducted until now to gain a more general understanding and general equations for the viscous force (Washino et al., 2017).

Capillary forces generally result from two different sources: surface tension σ and capillary pressure p_c (Fisher, 1926, Mazzone et al., 1987, Seville et al., 2000). The surface tension force $F_{\text{cap},\sigma}$ acts in the gas-solid-liquid contact line in the direction of contact angle θ. In a symmetric liquid bridge the tangential parts of the surface tension force at each point compensates the tangential force at the opposite point in the contact line, as can be seen in figure 1.6. Therefore, the resulting surface tension force only acts adhesively in normal direction. It can be calculated by the product of normal part of

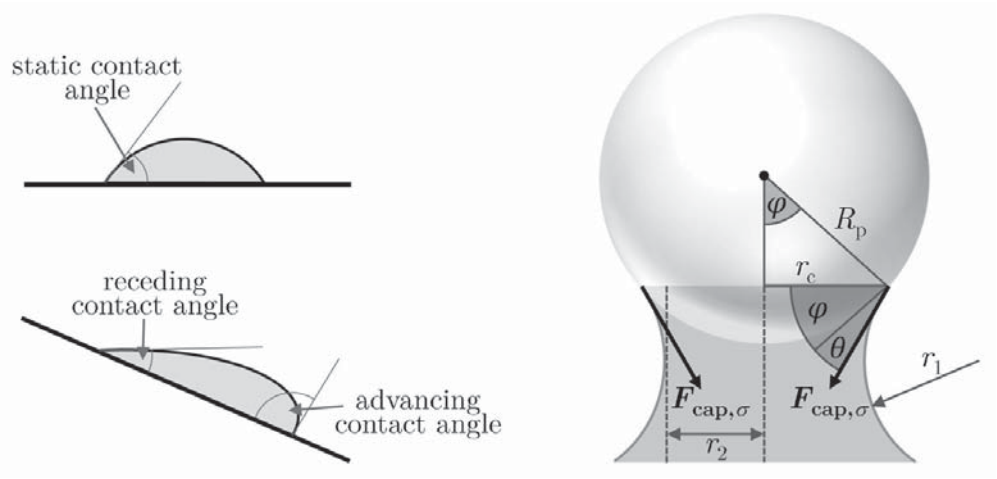

FIGURE 1.6: Comparison of different contact angles of a droplet on a wall (left) and direction of surface tension force and geometry of a capillary bridge attached to a spherical particle (right).

surface tension and length of the liquid-solid contact line ($2\pi r_c$). For a capillary bridge attached to a particle, as shown schematically in figure 1.6, this yields:

$$F_{cap,\sigma} = 2\pi r_c \sigma \sin(\theta + \varphi) \tag{1.16}$$

with φ as half-filling angle. Different contact angles θ are possible for a liquid bridge. In a static liquid bridge the so called static contact angle is crucial. Since the collision of a particle with a liquid layer is strongly dynamic the advancing and receding contact angles have to be taken into account. Figure 1.6 compares the different contact angles for a liquid droplet on a wall. During impact the advancing contact angle is present between liquid and particle, as can be seen in the second photo in figure 1.5. When the particle emerges from the liquid layer during rebound as well as during liquid bridge formation the receding contact angle is present (fourth and fifth image in figure 1.5). The second source of capillary effect is the capillary pressure p_c, which either has an adhesive or repulsive effect on the wetted area of the particle (πr_c^2). The capillary pressure represents the pressure difference between the inside and outside of the liquid volume and depends on the surface tension of the liquid and the geometry of the gas-liquid interface. It was mathematically defined in the Young-Laplace equation:

$$p_c = \sigma \left(\frac{1}{r_1} + \frac{1}{r_2} \right) \tag{1.17}$$

$$F_{cap,p} = \pi r_c^2 p_c \tag{1.18}$$

The exact curvature of a liquid bridge between two stationary particles or particle and wall would be that of a nodoid, which means, that it has a constant curvature (Rynhart, 2004). Since the exact geometry of capillary bridges is not easily solved analytically, in

literature different simplified or empirical models for the capillary force were developed. Typical simplifications of the geometry of the capillary bridge are the toroid approximation and parabolic approximation of the curvature. The most renown example of the toroid approximation is that by Fisher (1926), who correctly approximated the curvature of a liquid bridge between particles of equal size by circular arcs. This method was often taken over for similar (Simons et al., 1994) and slightly different geometric systems, such as liquid bridges between particle and wall (Clark et al., 1968, Kralchevsky and Nagayama, 2001) or particles of different size (Chen et al., 2011, Lian and Seville, 2016, Mehrotra and Sastry, 1980). Parabolic approximations assume the shape of the outer curvature to be parabolic and then the equation for capillary pressure (Pepin et al., 2000, Simons and Pepin, 2003) are solved analytically. Furthermore, several empirical models exist in literature. The empirical model for capillary forces most cited is that of Mikami et al. (1998). They used a regression analysis of numerical solutions for the capillary force to develop equations for liquid bridges between two equally sized particles as well as between particle and wall. The final correlations only depend on the volume of the liquid bridge, radius of the particle and surface tension of the liquid.

Most previous research regarding capillary forces focused on symmetric bridges and hydrophilic contact angles ($\theta < 90°$). Recently, some authors started looking into the influence of asymmetric bridge shapes (Cai and Bhushan, 2007, 2008b, Chau et al., 2007, Dodds et al., 2012, Marshall, 2014, Schade and Marshall, 2011) and hydrophobic contact angles ($\theta > 90°$) (Cai and Bhushan, 2008a,b).

When capillary bridges are investigated, also the critical length at which the bridge ruptures has to be addressed. Several correlations were formulated in literature, e.g. by Lian et al. (1993), Mikami et al. (1998) and Pitois et al. (2001). Typically, the critical rupture length of a static liquid bridge depends on bridge volume V_b and contact angle between liquid and particle. However, Pitois et al. (2001) extended the correlation of Lian et al. (1993) to dynamic liquid bridges by including the capillary number Ca into the equation for rupture length l_rupt:

$$l_\mathrm{rupt} = \left(1 + \frac{\theta}{2}\right) \cdot \left(1 + Ca^{1/2}\right) \cdot V_\mathrm{b}^{1/3} \tag{1.19}$$

$$Ca = \frac{v\eta}{\sigma} \tag{1.20}$$

Another important subject regarding capillary bridges is the amount of liquid transferred between the colliding bodies after rupture of the bridge. Much research is recently undergone to understand and describe the physical principles behind division of liquid between liquid bonded bodies. Some investigations and models already exist (Dodds et al., 2012, Matsuoka et al., 2012, 2016, Shi and McCarthy, 2008, Washino et al., 2016),